

## Electronic Supplementary Information

### Effect of the crystal structure of small precursor particles on the growth of $\beta$ -NaREF<sub>4</sub> (RE = Sm, Eu, Gd, Tb) nanocrystals

Benjamin Voß<sup>1</sup>, Jörg Nordmann<sup>1</sup>, Andreas Uhl<sup>2</sup>, Rajesh Kombar<sup>1</sup> and Markus Haase<sup>\*1</sup>

<sup>1</sup> Institute of Chemistry of New Materials, Osnabrück University, Germany - 49076 Osnabrück, Barbarastr.7

<sup>2</sup> Biomedizinische NMR Forschungs GmbH am Max-Planck-Institut für biophysikalische Chemie, 37070 Göttingen, Germany - Am Fassberg 11

Corresponding Author

\* markus.haase@uni-osnabrueck.de

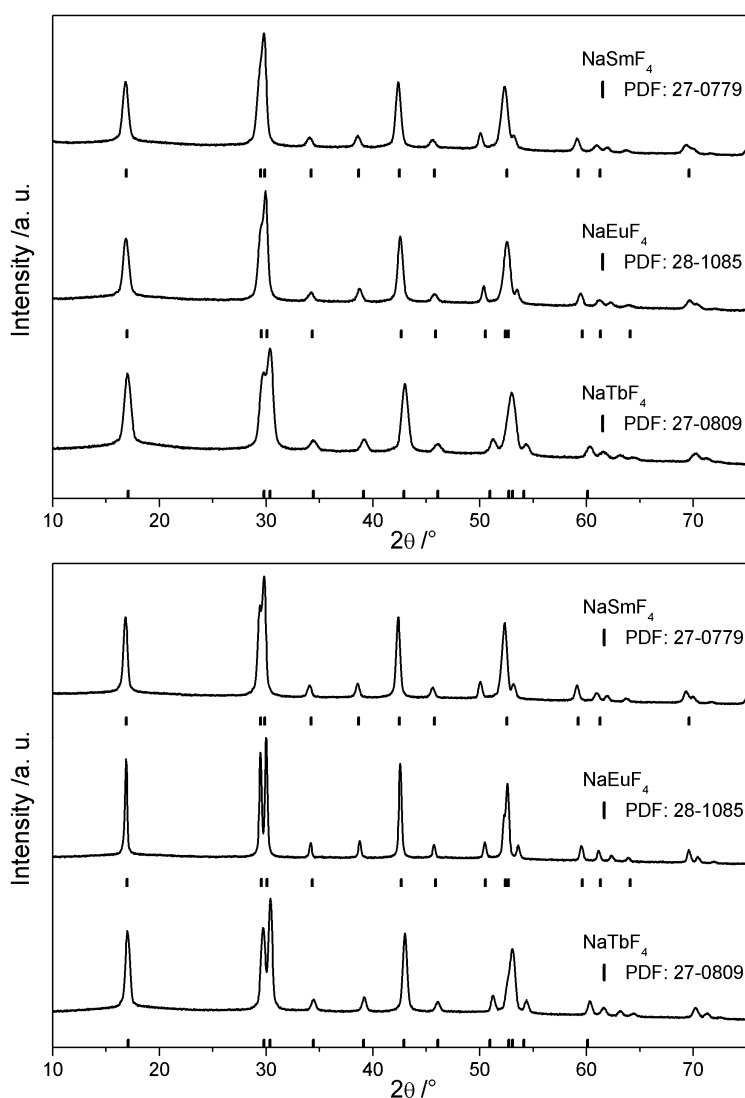


Figure S1. Powder diffraction patterns of product particles obtained by heating  $\beta$ -NaREF<sub>4</sub> (RE = Sm, Eu, Tb) precursor particles (top) and  $\alpha$ -NaREF<sub>4</sub> precursor particles (bottom) in oleic acid/octadecene. Vertical bars indicate the corresponding Bragg reflexes.

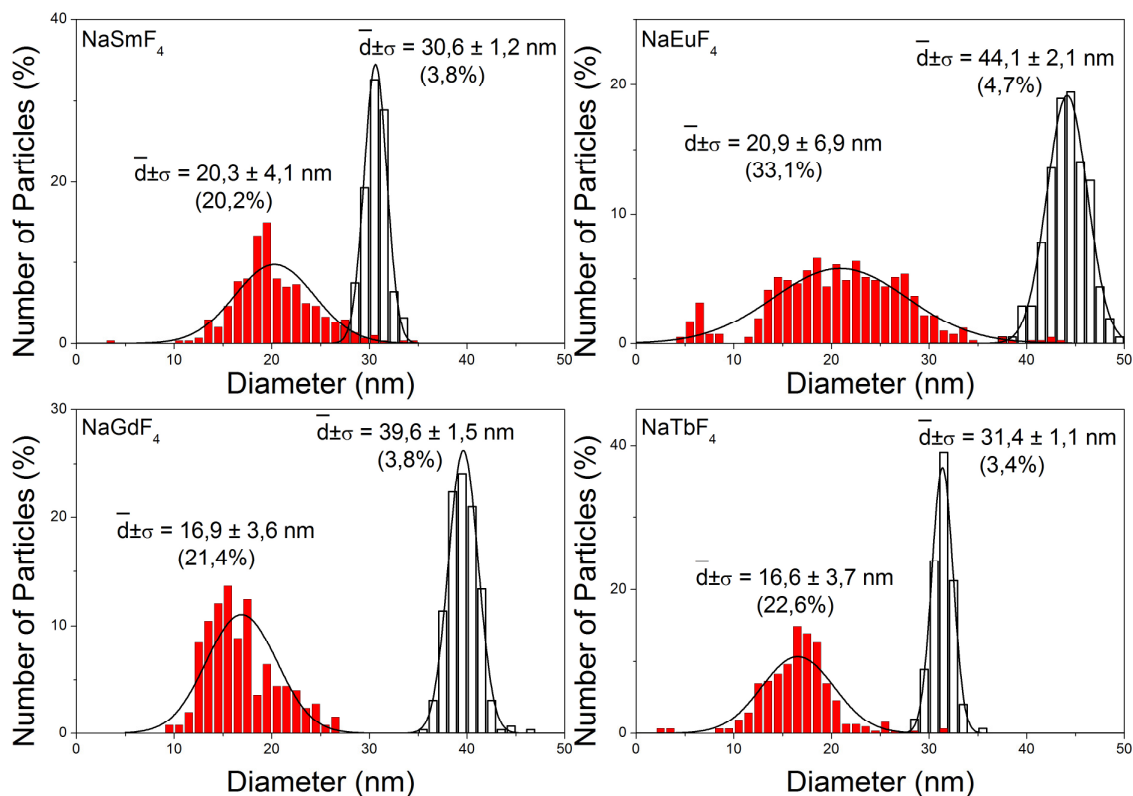


Figure S2. Particle size histograms of  $\beta$ - $\text{NaLnF}_4$  nanoparticles, as derived from TEM images, and values for the mean particle diameter, the standard deviation and the relative standard deviation (in %) as indicated. In all cases, the  $\beta$ -phase particles prepared from  $\alpha$ -phase precursor particles (white histograms) display more narrow particle size distributions and larger mean diameters than particles prepared from  $\beta$ -phase precursor particles (red histograms). The diameter given for the elongated  $\beta$ -phase particles (red histograms) corresponds to the diameter of a sphere with identical volume, assuming cylindrical shape of the elongated particles. Solid lines indicate Gauss Fits of the corresponding histograms.

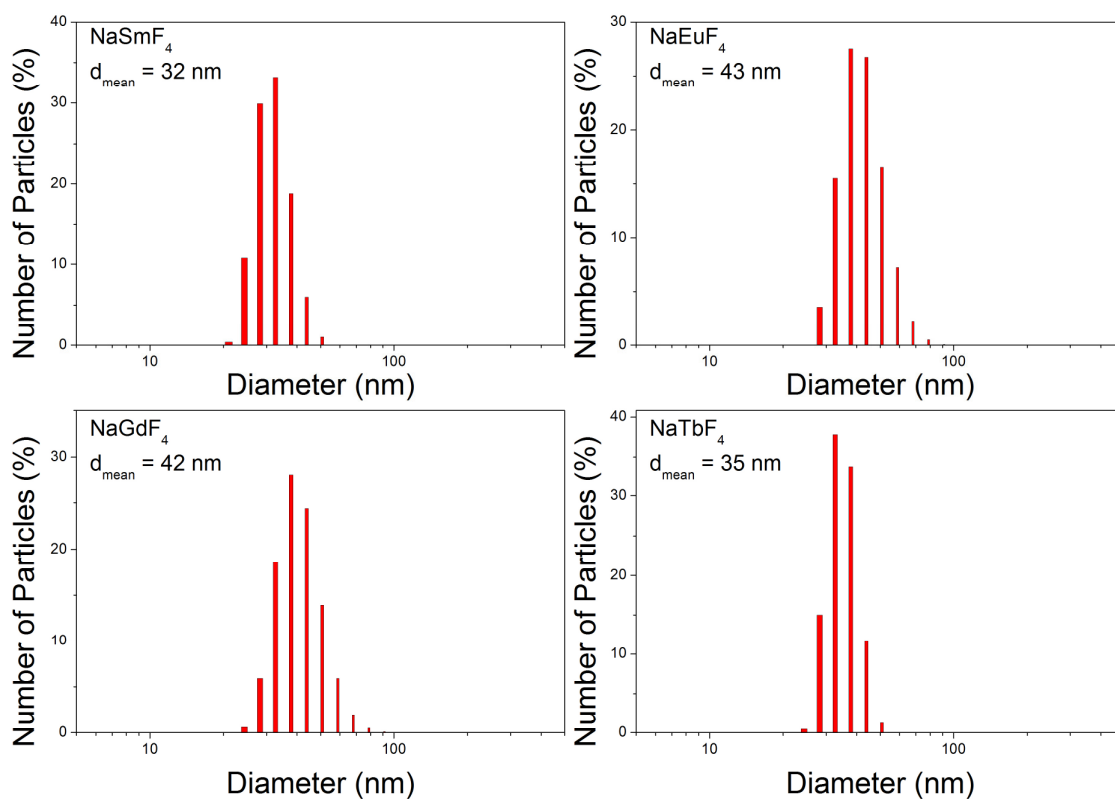


Figure S3. Dynamic light scattering data of  $\beta$ - $\text{NaLnF}_4$  nanoparticles prepared from  $\alpha$ -phase precursor particles. The mean hydrodynamic diameters observed in hexane solution are in accord with the TEM data, indicating that the particles are well dispersed.

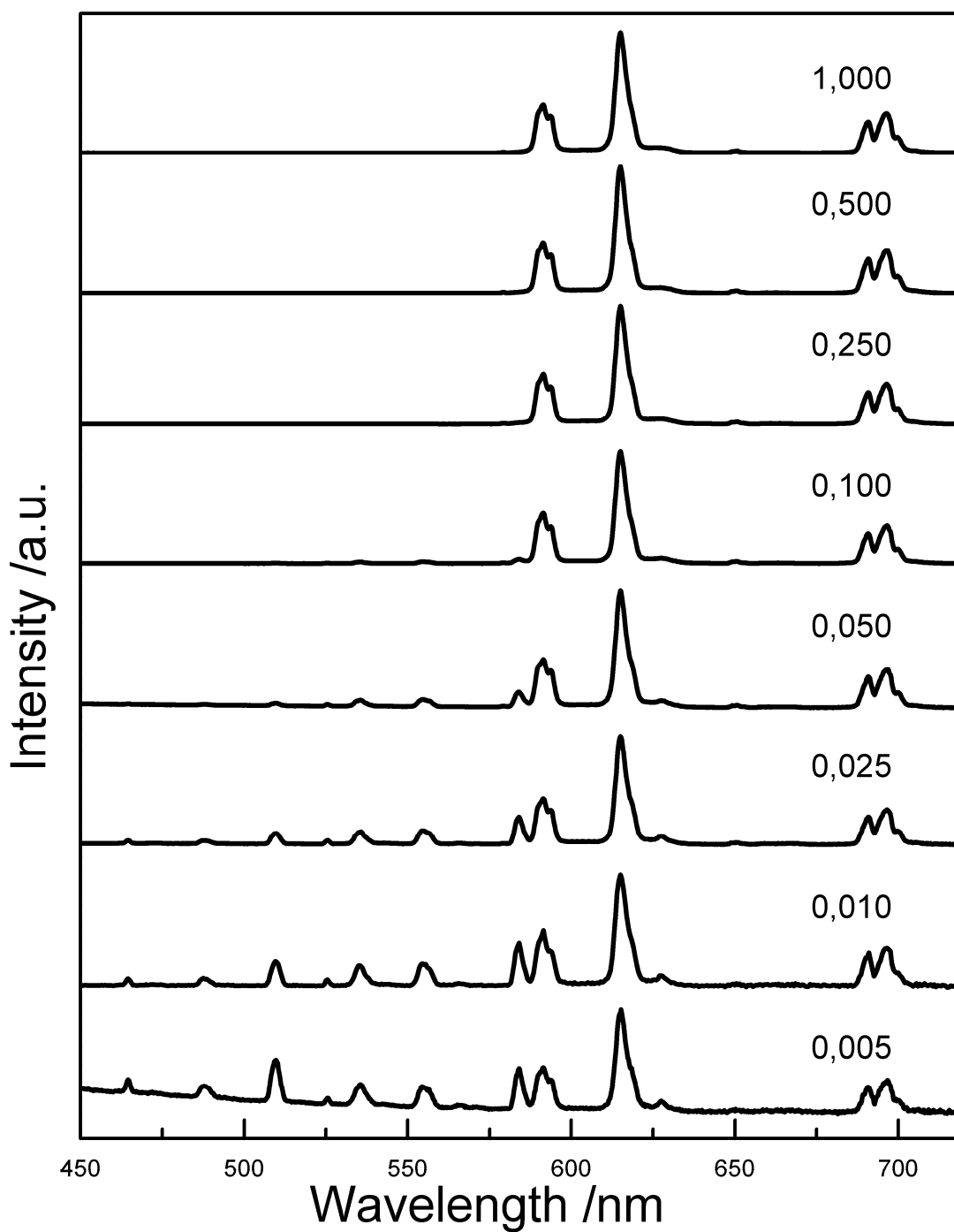


Figure S4. Emission spectra of NaGd<sub>1-x</sub>Eu<sub>x</sub>F<sub>4</sub> product particles with different Eu<sup>3+</sup> content. Due to cross-relaxation between neighboring Eu<sup>3+</sup> ions, the intensity ratio of the <sup>3</sup>D<sub>0</sub> → <sup>7</sup>F<sub>1</sub> to the <sup>3</sup>D<sub>0</sub> → <sup>7</sup>F<sub>2</sub> transitions depends on the molar fraction x of Eu<sup>3+</sup> given at each spectrum.

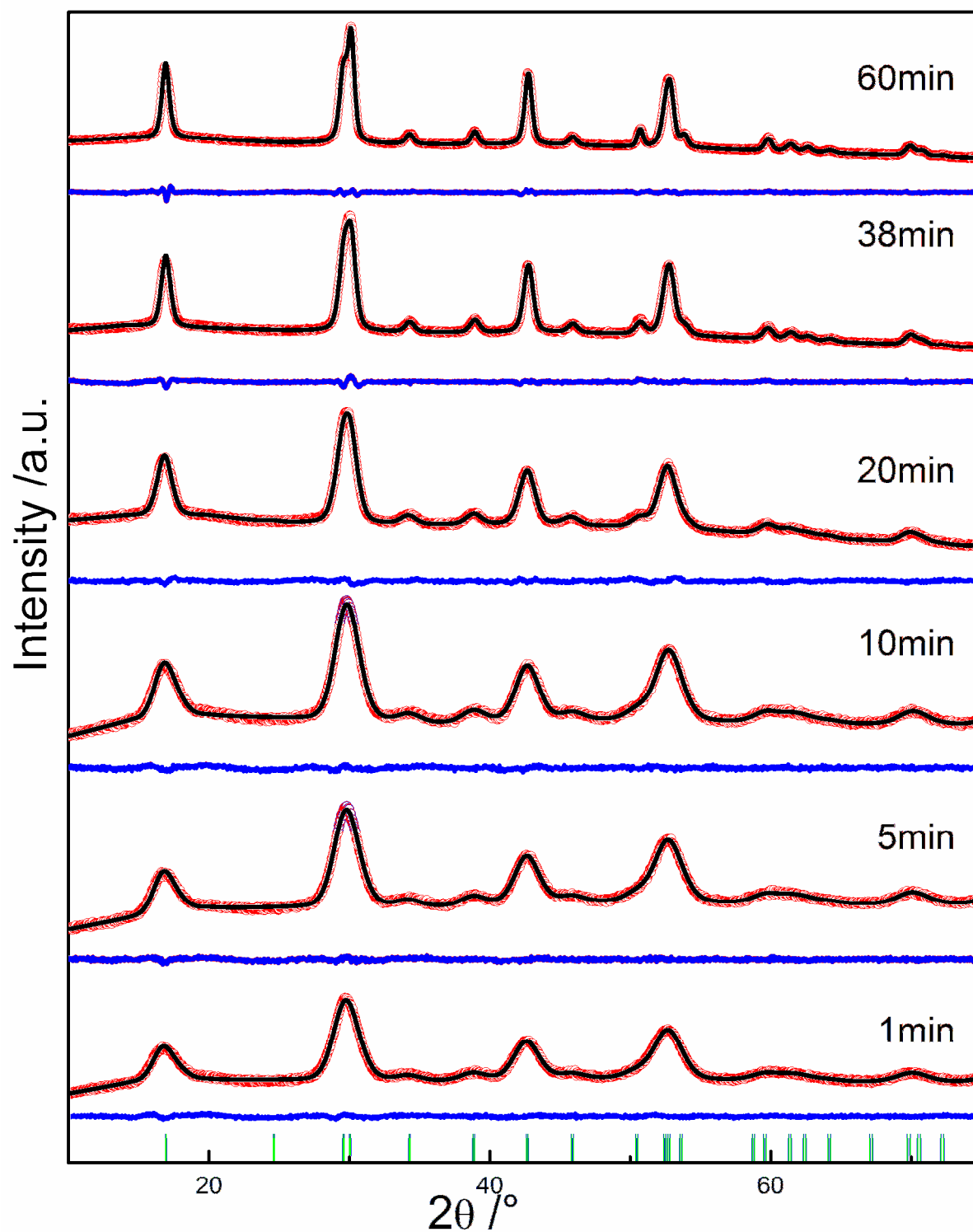


Figure S5a. XRD patterns of  $\beta$ -phase NaGdF<sub>4</sub> particles after different heating times at 320 °C and Rietveld fits of the XRD data used to calculate the mean particle sizes given in Figure 5.

Table S1a. Lattice constants and other parameters derived from Rietveld fits of the XRD data of the series of  $\beta$ -NaGdF<sub>4</sub> particles given in Figure 5 (Cu K $\alpha$  radiation, 40 kV, 40 mA,  $\lambda = 1.54\text{\AA}$ )

Reaction time (min)	1	5	10	20	38	60
mean crystallite size (nm) (010)*(001)	3,5	3,9	4,2	6,4	10,5	12*22
space group	P-6	P-6	P-6	P-6	P-6	P-6
a ( $\text{\AA}$ )	6,0455	6,0232	6,0478	6,0532	6,0369	6,0384
c ( $\text{\AA}$ )	3,6189	3,6093	3,6167	3,6027	3,6000	3,6004
V /Z ( $\text{\AA}^3$ )	114,543	113,398	114,562	114,322	113,623	113,69
Z	1	1	1	1	1	1
number of reflections	28	28	28	28	28	28
global refined parameters	9	10	9	10	9	10
Profile refined parameters	8	8	8	8	8	8
int. affect. refined parameters	1	2	2	1	1	1
$R_p$ <sup>[a]</sup>	7,90	11,6	8,02	9,27	9,4	8,35
$R_{wp}$ <sup>[b]</sup>	6,59	9,64	6,52	6,89	6,79	6,13
$R_{exp}$ <sup>[c]</sup>	4,87	8,25	4,94	4,46	3,90	3,56
$\chi^2$	1,83	1,36	1,75	2,39	3,04	2,96
$R_f$ <sup>[d]</sup>	1,16	1,26	1,30	2,09	1,44	1,23
Bragg R factor <sup>[e]</sup>	1,45	1,31	1,84	1,88	1,61	1,19

[a]  $R_p = (\sum |Y_o - Y_c| / \sum Y_o) * 100$ , [b]  $R_{wp} = ((\sum w(Y_o - Y_c)^2 / \sum w Y_o^2)^{1/2}) * 100$ , [c]  $R_{exp} = ((n-p) / \sum w Y_o^2)^{1/2} * 100$ ,

[d]  $R_f = (\sum |F_o' - F_c| / \sum |F_o|) * 100$ , [e] Bragg  $R_b = (\sum |Y_o - Y_c| / \sum |Y_o|) * 100$  (Reliability factors for points with Bragg contribution)

All Rietveld fits of  $\beta$ -phase NaGdF<sub>4</sub> nanocrystals are based on the crystal information file ICSD 415868. For the cubic  $\alpha$ -NaGdF<sub>4</sub> nanocrystals the ICSD file 60257 of cubic  $\alpha$ -NaYF<sub>4</sub> was modified according to PDF 27-0698.

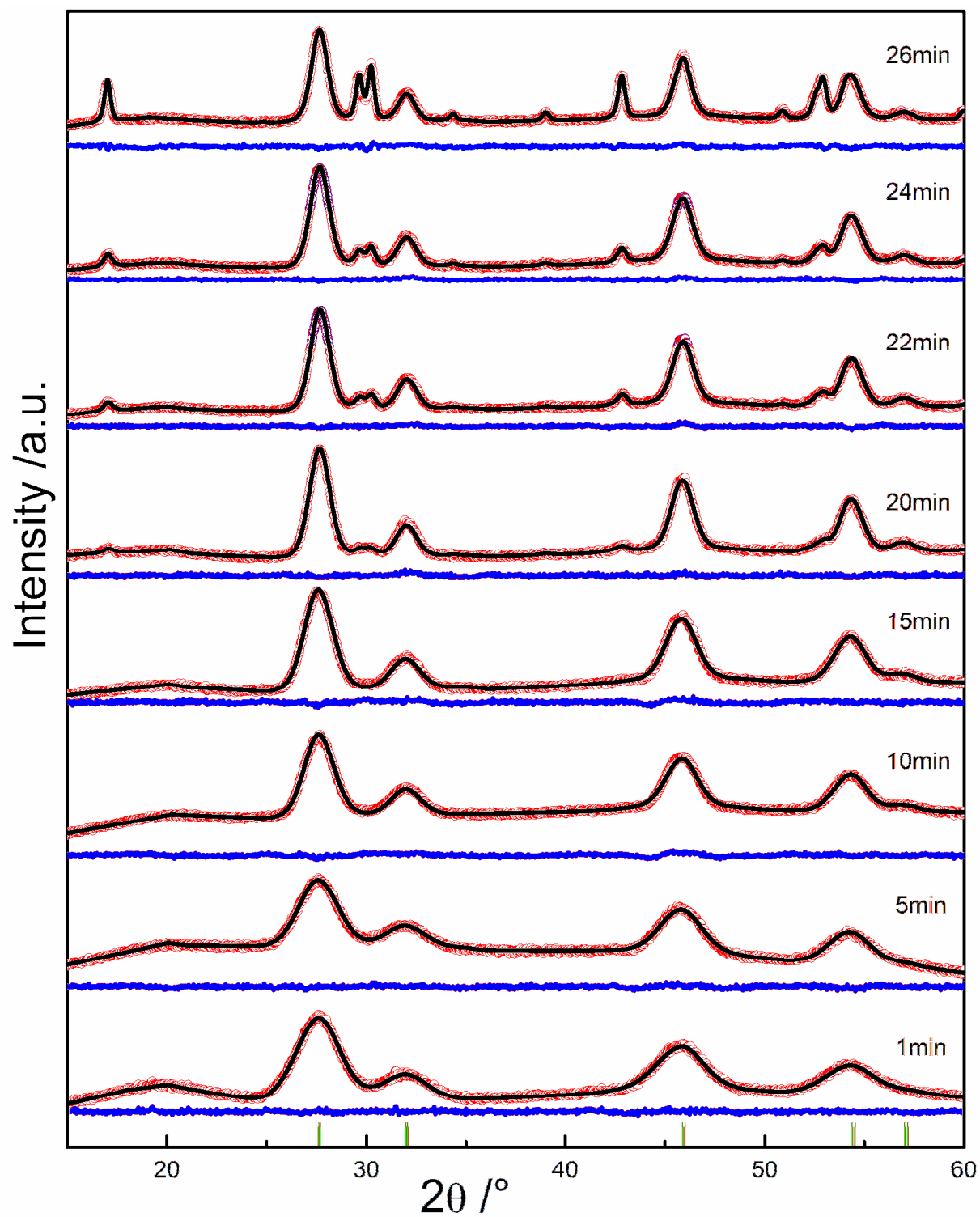


Figure S5b. XRD patterns of  $\alpha$ -phase NaGdF<sub>4</sub> particles after different heating times at 320 °C and Rietveld fits of the XRD data used to calculate the mean particle sizes given in Figure 5 and 7.

Table S1b. Lattice constants and other parameters derived from Rietveld fits of the XRD data of the  $\alpha$ -NaGdF<sub>4</sub> particles given in Figure 5 and 7 (Cu K $\alpha$  radiation, 40 kV, 40 mA,  $\lambda = 1.54 \text{ \AA}$ )

Reaction time (min)		1	5	10	15	20	22	24	26
mean crystallite size (nm) (010)*(001)	$\alpha$	3	3,6	4,6	5	6,9	7,2	7,3	8,4
	$\beta$					9,7	13*15	15*17	25*25
space group	$\alpha$	FM-3M	FM-3M	FM-3M	FM-3M	FM-3M	FM-3M	FM-3M	FM-3M
	$\beta$					P-6	P-6	P-6	P-6
a (Å)	$\alpha$	5,5902	5,5985	5,5926	5,5925	5,5915	5,5920	5,5920	5,5912
	$\beta$					6,0221	6,0297	6,0298	6,0292
c (Å)	$\alpha$	5,5902	5,5985	5,5926	5,5925	5,5916	5,5920	5,5920	5,5912
	$\beta$					3,5937	3,5857	3,5857	3,5870
V /Z (Å <sup>3</sup> )	$\alpha$	174,70	175,48	174,93	174,912	174,82	174,86	174,864	174,79
	$\beta$					112,87	112,90	112,903	112,92
Z	$\alpha$	2	2	2	2	2	2	2	2
	$\beta$					1	1	1	1
number of reflections		8	5	7	7	21	21	21	21
global r. p.		14	14	13	15	14	14	14	14
Profile r. p.		8	8	8	5	16	17	17	17
int. affect. r. p.		1	0	1	0	2	3	3	1
$R_p$ [a]		9,18	10,3	13,2	13,4	9,25	8,1	7,79	10,5
$R_{wp}$ [b]		7,3	8,08	8,93	8,45	6,5	5,78	5,59	7,76
$R_{exp}$ [c]		6,15	6,66	5,8	6,39	5,42	4,49	4,49	4,68
$\chi^2$		1,41	1,47	2,37	1,75	1,44	1,66	1,55	2,75
$R_f$ [d]	$\alpha$	0,758	0,377	1,39	1,22	0,869	0,681	0,76	0,859
	$\beta$					3,44	2,2	1,88	1,55
Bragg R factor [e]	$\alpha$	0,751	0,563	2	1,58	0	1,2	1,32	1,77
	$\beta$					3,57	2,46	2,24	2,23
$\beta$ -Phase fraction						11,24%	14,44%	16,67%	34,62%

r. p. (refined parameters), [a]  $R_p = (\sum |Y_o - Y_c| / \sum Y_o) * 100$ , [b]  $R_{wp} = ((\sum w(Y_o - Y_c)^2 / \sum w Y_o^2)^{1/2}) * 100$ , [c]  $R_{exp} = ((n-p) / \sum w Y_o^2)^{1/2} * 100$ ,

[d]  $R_f = (\sum |F_o' - F_c| / \sum |F_o|) * 100$ , [e] Bragg  $R_b = (\sum |Y_o - Y_c| / \sum |Y_o|) * 100$  (Reliability factors for points with Bragg contribution)

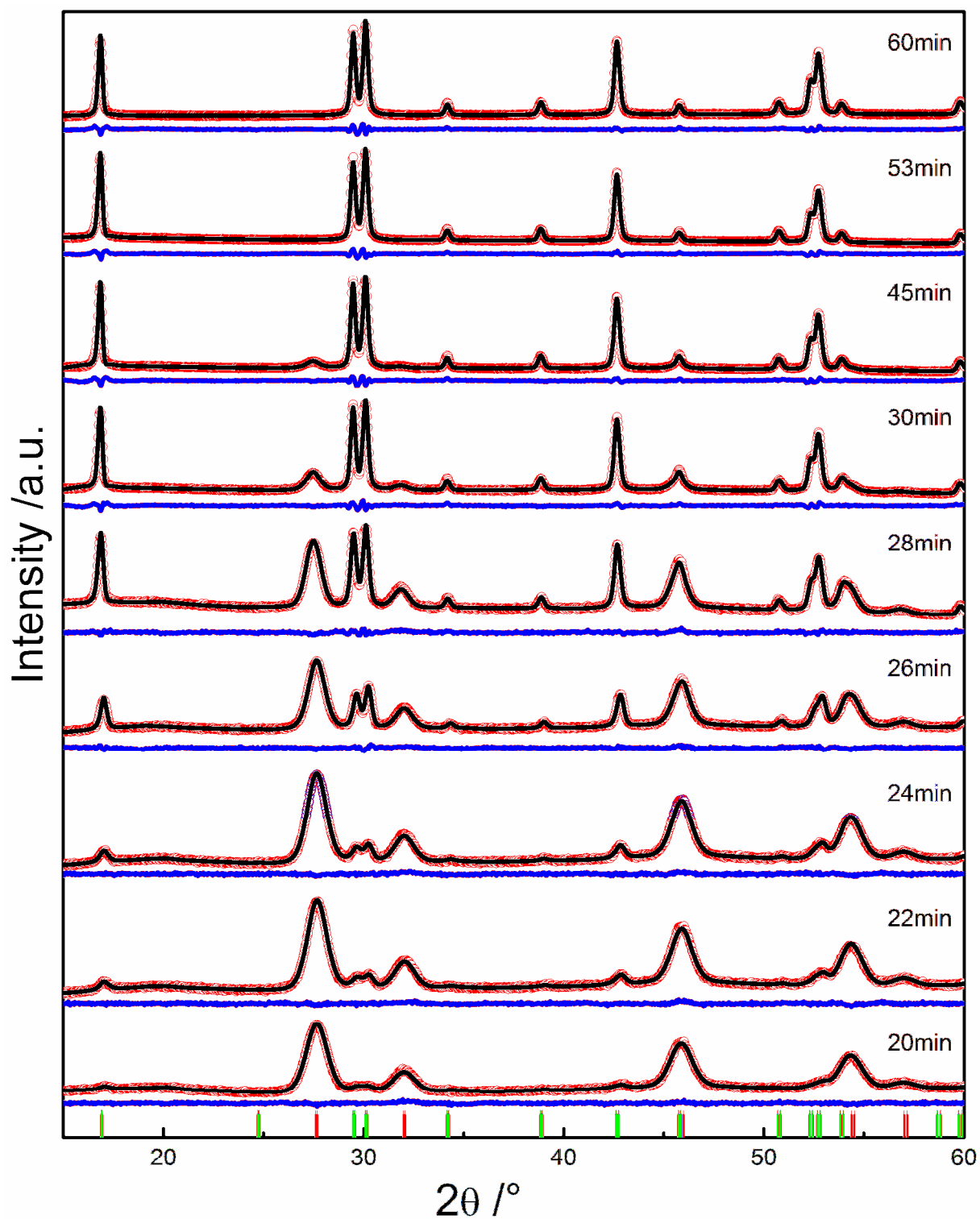


Figure S6. XRD patterns of  $\alpha$ -phase NaGdF<sub>4</sub> particles after different heating times at 320 °C including the Rietveld fits used to calculate the molar fraction of the  $\alpha$ -phase and the mean particle sizes given in Figure 7.



Table S2. Lattice constants and other parameters derived from Rietveld fits of the XRD data of the  $\alpha$ -NaGdF<sub>4</sub> particles given in Figure 7 (Cu K $\alpha$  radiation, 40 kV, 40 mA,  $\lambda = 1.54 \text{ \AA}$ )

Reaction time (min)		28	30	45	53	60
mean crystallite size (nm) (010)*(001)	$\alpha$	9,7	9,54	8,48		
	$\beta$	31,5*29,7	39,9*33,5	42,8*35,2	41,9*39,4	46,6*38,0
space group	$\alpha$	FM-3M	FM-3M	FM-3M		
	$\beta$	P-6	P-6	P-6	P-6	P-6
a (Å)	$\alpha$	5,5613	5,6130	5,6128		
	$\beta$	6,0536	6,0566	6,0563	6,0565	6,0559
c (Å)	$\alpha$	5,5613	5,6130	5,6128		
	$\beta$	3,5972	3,5982	3,5986	3,5984	3,5987
V / Z (Å <sup>3</sup> )	$\alpha$	176,85	176,85	176,83		
	$\beta$	114,162	114,307	114,31	114,31	114,29
Z	$\alpha$	1	1	1		
	$\beta$	2	2	2	2	2
number of reflections		36	36	36	28	
global r. p.		14	9	9	9	
Profile r. p.		15	16	17	9	
int. affect. r. p.		3	1	2	2	
$R_p$ [a]		10,5	11,1	11,1	11,4	11,7
$R_{wp}$ [b]		7,18	7,6	7,91	7,55	7,59
$R_{exp}$ [c]		5,04	4,01	3,43	3,17	3,50
$\chi^2$		2,03	3,58	5,31	5,66	4,77
$R_f$ [d]	$\alpha$	2,29	4,18	5,22		
	$\beta$	2,17	2,46	2,69	2,60	3,00
Bragg R factor [e]	$\alpha$	3,02	4,45	5,79		
	$\beta$	1,73	2,55	2,58	2,20	2,42
$\beta$ -Phase fraction		54,01%	80,13%	90,88%	100%	100%

r. p. (refined parameters), [a]  $R_p = (\sum |Y_o - Y_c| / \sum Y_o) * 100$ , [b]  $R_{wp} = ((\sum w(Y_o - Y_c)^2) / \sum w Y_o^2)^{1/2} * 100$ , [c]  $R_{exp} = ([n-p] / \sum w Y_o^2)^{1/2} * 100$ ,

[d]  $R_f = (\sum |F_o' - F_c| / \sum |F_o|) * 100$ , [e] Bragg  $R_b = (\sum |Y_o - Y_c| / \sum |Y_o|) * 100$  (Reliability factors for points with Bragg contribution)

Table S3. Preparation of Rare earth oleates of group II

	Samarium	Europium	Terbium
RECl <sub>3</sub> [g]	7,296	21,985	7,468
M <sub>(RECl<sub>3</sub>)</sub> [g/mol]	364,811	366,415	373,376
n <sub>(RECl<sub>3</sub>)</sub> [mmol]	20	60	20
M <sub>(RE-Oleate)</sub> [g/mol]	994,72	996,324	1003,29
Na-Oleate [g]	18,267	54,801	18,267
Water [ml]	30	90	30
Ethanol [ml]	40	120	40
Hexane [ml]	70	210	70

Table S4. Weighted amounts of NaREF<sub>4</sub> precursor particles (RE = Sm, Eu, Gd, Tb) for the synthesis of the final products particles

precursor particles	[g]
NaSmF <sub>4</sub>	1,247
NaEuF <sub>4</sub>	1,255
NaGdF <sub>4</sub>	1,281
NaTbF <sub>4</sub>	1,290

Table S5. Weighted amounts of NaGdF<sub>4</sub> and NaEuF<sub>4</sub> precursor particles for the synthesis of mixed NaGd<sub>x-1</sub>Eu<sub>x</sub>F<sub>4</sub> product particles

x	NaGdF <sub>4</sub> [g]	NaEuF <sub>4</sub> [g]
0,01	1,268	0,0125
0,05	1,217	0,0627
0,1	1,153	0,1255